Determination of the telescope nodding reproducibility of the OD 858 pointing programme after the ACMS/STR two-dimensional focal length parameter update

M. Nielbock and U. Klaas

Max-Planck-Institut für Astronomie,
Königstuhl 17, D-69117 Heidelberg, Germany

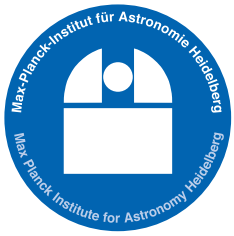

Contents

1 Preface

1.1 Document History

Version	Date	Author(s)	Change description
1.0	7th October 2011	M. Nielbock, U. Klaas (MPIA)	initial version

1.2 References

Reference document	Date	Document ID	
Herschel Observers' Manual	31-Mar-2011	HERSCHEL-HSC-DOC-0876	(RD1)
Herschel Pointing Calibration Plan	05-Aug-2008	HERSCHEL-HSC-DOC-1139	(RD2)
Herschel pointing accuracy and calibration procedures	05-Dec-2003	SCI-PT-19552	(RD3)
SMPS – Pointing Modes	01-Oct-2010	HERSCHEL-HSC-DOC-624	(RD4)
PACS Pointing Calibration Sources	26-Feb-2010	PICC-MA-TN-003	(RD5)
Gyro Nodding Pointing Mode (aka CP Raster): Performance Test 1 with PACS Photometer - Performance comparison with fine pointing mode on OD 516	25-Mar-2011	PICC-MA-TR-091	(RD6)
Gyro Nodding Pointing Mode (aka CP Raster): Performance Test 2 with PACS Photometer on OD 649	25-Mar-2011	PICC-MA-TR-093	(RD7)
Pointing calibration status after STR 2D update	05-Oct-2011	HERSCHEL-HSC-DOC-1880	(RD8)

1.3 Observations

Target	OBSID	AOR label
HIP 36675	1342228855	ObsCal_RP_FPG_PPhot_Blue_cycle48_OD858_HIP36675
HIP 30343	1342228856	ObsCal_RP_FPG_PPhot_Blue_cycle48_OD858_HIP30343
HIP 28041	1342228857	ObsCal_RP_FPG_PPhot_Blue_cycle48_OD858_HIP28041
HIP 30520	1342228866	ObsCal_RP_FPG_PPhot_Blue_cycle48_OD858_HIP30520
HIP 36288	1342228867	ObsCal_RP_FPG_PPhot_Blue_cycle48_OD858_HIP36288
HIP 30945	1342228868	ObsCal_RP_FPG_PPhot_Blue_cycle48_OD858_HIP30945

continued.

Target	OBSID	AOR label
HD 39741	1342228869	ObsCal_RP_FPG_PPhot_Blue_cycle48_OD858_HD39741
HIP 75847	1342228870	ObsCal_RP_FPG_PPhot_Blue_cycle48_OD858_HIP75847
HIP 80802	1342228871	ObsCal_RP_FPG_PPhot_Blue_cycle48_OD858_HIP80802
HIP 83866	1342228872	ObsCal_RP_FPG_PPhot_Blue_cycle48_OD858_HIP83866
HIP 81835	1342228873	ObsCal_RP_FPG_PPhot_Blue_cycle48_OD858_HIP81835
HIP 78574	1342228874	ObsCal_RP_FPG_PPhot_Blue_cycle48_OD858_HIP78574
HIP 80704	1342228875	ObsCal_RP_FPG_PPhot_Blue_cycle48_OD858_HIP80704
HIP 77501	1342228876	ObsCal_RP_FPG_PPhot_Blue_cycle48_OD858_HIP77501
HIP 78235	1342228877	ObsCal_RP_FPG_PPhot_Blue_cycle48_OD858_HIP78235
HIP 79233	1342228878	ObsCal_RP_FPG_PPhot_Blue_cycle48_OD858_HIP79233
HIP 80488	1342228879	ObsCal_RP_FPG_PPhot_Blue_cycle48_OD858_HIP80488
HIP 87747	1342228880	ObsCal_RP_FPG_PPhot_Blue_cycle48_OD858_HIP87747
HIP 84346	1342228881	ObsCal_RP_FPG_PPhot_Blue_cycle48_OD858_HIP84346
HIP 87538	1342228882	ObsCal_RP_FPG_PPhot_Blue_cycle48_OD858_HIP87538
HIP 84780	1342228883	ObsCal_RP_FPG_PPhot_Blue_cycle48_OD858_HIP84780
HIP 79593	1342228884	ObsCal_RP_FPG_PPhot_Blue_cycle48_OD858_HIP79593
HIP 84071	1342228889	ObsCal_RP_FPG_PPhot_Blue_cycle48_OD858_HIP84071
HIP 82912	1342228890	ObsCal_RP_FPG_PPhot_Blue_cycle48_OD858_HIP82912
HIP 77023	1342228891	ObsCal_RP_FPG_PPhot_Blue_cycle48_OD858_HIP77023
HIP 76377	1342228892	ObsCal_RP_FPG_PPhot_Blue_cycle48_OD858_HIP76377
HIP 82273	1342228893	ObsCal_RP_FPG_PPhot_Blue_cycle48_OD858_HIP82273
PPM 787044	1342228894	ObsCal_RP_FPG_PPhot_Blue_cycle48_OD858_PPM787044
HIP 68815	1342228895	ObsCal_RP_FPG_PPhot_Blue_cycle48_OD858_HIP68815
HIP 61404	1342228896	ObsCal_RP_FPG_PPhot_Blue_cycle48_OD858_HIP61404
HIP 55355	1342228897	ObsCal_RP_FPG_PPhot_Blue_cycle48_OD858_HIP55355
HIP 46806	1342228898	ObsCal_RP_FPG_PPhot_Blue_cycle48_OD858_HIP46806
HIP 19424	1342228899	ObsCal_RP_FPG_PPhot_Blue_cycle48_OD858_HIP19424
HIP 31057	1342228900	ObsCal_RP_FPG_PPhot_Blue_cycle48_OD858_HIP31057
HIP 30438	1342228901	ObsCal_RP_FPG_PPhot_Blue_cycle48_OD858_HIP30438
HIP 37819	1342228902	ObsCal_RP_FPG_PPhot_Blue_cycle48_OD858_HIP37819
HIP 35264	1342228903	ObsCal_RP_FPG_PPhot_Blue_cycle48_OD858_HIP35264
HD 43635	1342228904	ObsCal_RP_FPG_PPhot_Blue_cycle48_OD858_HD43635
HIP 28874	1342228905	ObsCal_RP_FPG_PPhot_Blue_cycle48_OD858_HIP28874
HIP 28816	1342228906	ObsCal_RP_FPG_PPhot_Blue_cycle48_OD858_HIP28816
HIP 30800	1342228907	ObsCal_RP_FPG_PPhot_Blue_cycle48_OD858_HIP30800
HIP 30326	1342228915	ObsCal_RP_FPG_PPhot_Blue_cycle48_OD858_HIP30326
HIP 32923	1342228916	ObsCal_RP_FPG_PPhot_Blue_cycle48_OD858_HIP32923

1.4 Acronyms

ACMS	Attitude Control and Measurement System
APE	Absolute Pointing Error
PACS	Photodetector Array Camera and Spectrograph
RPE	Relative Pointing Error
SRPE	Spatial Relative Pointing Error
STR	Star Tracker

2 Introduction and motivation

On average, the pointing performance showed acceptable results during the first half of the mission. However, a number of outliers was flagged that appeared to be inconsistent with the statistical uncertainties and to show some systematics. After a thorough investigation, it turned out that the focal length parameter used by the ACMS to determine the telescope pointing did not reflect the spatial scale of the STR cameras. The situation was obviously aggravated by the reduction of the STR camera temperature. This mismatch led to particularly large outliers in cases when the guide star pattern observed by the STR was highly asymmetric.

A first modification of the ACMS concerned the update of the one-dimensional focal length parameter done on OD 762 that resulted in an improvement of the overall pointing accuracy. Nevertheless, an additional two-dimensional parameter update was suggested and tested on OD 858 which led to a substantial reduction of the pointing uncertainties with an APE below 1″ (RD8). The change was made permanent on OD 866.

Apart from the APE, also the RPE, the SRPE and the nod throw stability are crucial parameters of the pointing performance. This is of particular importance for chopped/nodded observations done with the PACS spectrometer. A poor SRPE or nodding reproducibility is a main contribution to the uncertainties in recovering line fluxes and line profiles. A dedicated programme to evaluate the CP raster pointing mode in terms of an improved nodding reproducibility was unsuccessful. In light of these issues, we were eager to learn, whether the updates of the ACMS also provided a benefit for the nodding performance. Therefore, observations performed on OD 858 to assess the pointing performance after the two-dimensional ACMS/STR update were analysed by measuring the nodding throws and the pointing stability on the nod positions.

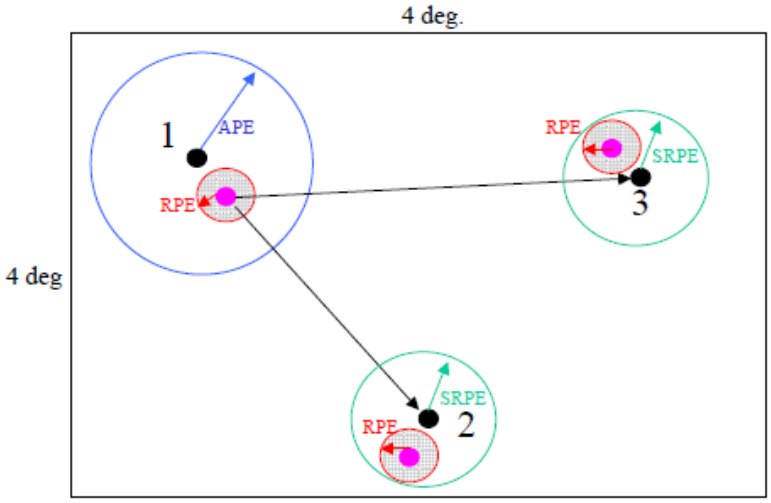

Figure 1: Illustration of the APE, the RPE, and the SRPE and their definitions. The initial commanded direction (black dot no 1) is achieved within the APE accuracy (blue circle). The actual pointing of the spacecraft (dotted area within red circle) has an average direction (purple dot). New directions are commanded (black dot 2+3) relative to the initial actual direction (purple dot 1) and are met within the SRPE requirement. The SRPE applies for raster pointing and raster with an offset. However for consecutive inertial fixed pointings, the SRPE does not apply (RD3).

Formally, the SRPE only applies to observations using pointing modes that include relative offsets to a reference coordinate, i.e. *basic_raster_pointing*, *raster_pointing*, *nodding_raster_pointing*, and *nodding_of_raster_pointing* (RD3). However, the chop/nod observations done with the PACS instrument, both the photometer and the spectrometer, are done with *basic_fine_pointing*, where the positions of the nod positions are attributed to fixed celestial coordinates. So, internally, the nodding is a sequence of two individual pointing requests. Hence, it is not the SRPE but the APE that determines the nodding performance. However, one might argue that the small displacements of less than 3′ involved in the currently implemented version of the chopped/nodded observations would have a smaller effect on the pointing uncertainty. Therefore, for this report, we define a pseudo SRPE (pSRPE) as the APE for small displacements as used during chopped/nodded observations.

As a result, the nod throw can be used as a proxy for the pSRPE. The reproducibility of the nod throw is a result of both the RPE and the pSRPE, because it is a superposition of the capability to accurately move the telescope between two positions and the stability of the pointing on one nod position. Since the RPE turns out to be a negligible contribution in comparison to the overall uncertainty, it can be taken as a representative measure of the pSRPE.

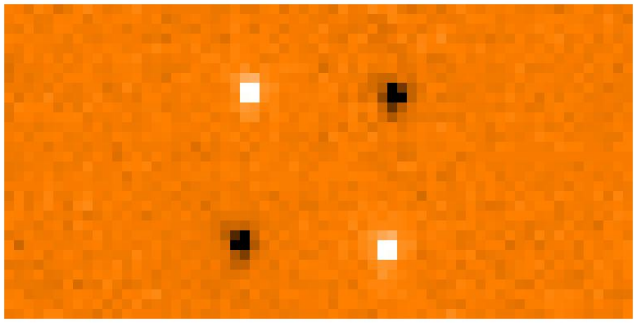

Figure 2: Typical image pattern of a nodding cycle of a chopped PACS photometer observation after subtracting the frames of the two chop and the two nod positions. The chopping is done along the S/C y axis (horizontal), while the nodding is done along the S/C z axis (vertical). After subtracting the individual frames, the target is seen twice as a positive and twice as a negative signal.

3 Observations and data reduction

The pointing programme consisted of 43 chopped/nodded observations with the PACS photometer (see Sect. 1.3). Each observation consists of an AB nod cycle pattern carried out with the *basic_fine_pointing* pointing mode (RD4). A given nod position contains a chop cycle with three different offsets around the nominal chop throw for dithering. The chopping and dithering is done along the S/C y axis using the internal focal plane chopper, while the nodding is done with the telescope along the S/C z axis. The target selection was based on the list given in RD5.

The data were processed by a dedicated HIPE script that performs the usual data reduction scripts up to Level 1 and produces maps in the instrument reference frame as shown in Fig. 2. The actual nod throw was calculated by fitting the target positions for each of the six resulting images of the star for the three dither positions per nod position and transforming these numbers into the S/C reference frame.

4 Results

Table 2 lists the mean nod throw and its standard deviation for each observation. Since there are six measurements per observation, the standard deviation σ_{off} (Eq. 2) of the total offset off (Eq. 1) attained for one observation can be interpreted as the RPE. As an example, the evolution of the offsets during the observation 1342228869 is listed in Tab. 1. In this case, the reproducibility for a certain nod position ranges between $0.10''$ and $0.21''$. As a result, the reproducibility of the nod throw θ amounts to $0.27''$. This is very important for the stability during PACS spectrometer observations, where it determines the accuracy of the total flux measured within a certain spatial module.

$$off = \sqrt{\Delta y^2 + \Delta z^2} \quad (1)$$

$$\sigma_{off} = \frac{\sqrt{(\sigma_{\Delta y}\Delta y)^2 + (\sigma_{\Delta z}\Delta z)^2}}{off} \quad (2)$$

Table 1: Evolution of nod positions and of nod throws θ per chop cycle during the observation with the OBSID 1342228906, all in arcseconds.

	Nod A		Nod B		
Measurement	Δy	Δz	Δy	Δz	θ
1	1.11	25.90	0.61	-24.86	50.76
2	0.87	26.11	0.76	-25.05	51.16
3	0.81	25.91	0.13	-24.48	50.39
4	0.69	26.01	0.57	-24.71	50.72
5	0.99	25.87	0.26	-24.51	50.39
6	0.88	26.12	0.47	-24.75	50.86
Mean	0.89	25.99	0.47	-24.73	50.71
σ	0.13	0.10	0.21	0.20	0.27

The scatter of the mean of nod throws of all pointing observations can be regarded as a good estimate of the pSRPE. The combination of a series of observations is comparable to a long single observation with a large number of nod cycles. However, this scatter is only an approximation to the pSRPE, because the nod throw is also influenced by the pointing stability, the RPE. These results are visualised in Fig. 3 which gives a statistical overview of the nod throws achieved during the 43 individual measurements. The mean and the rms of the entire distribution are added, too.

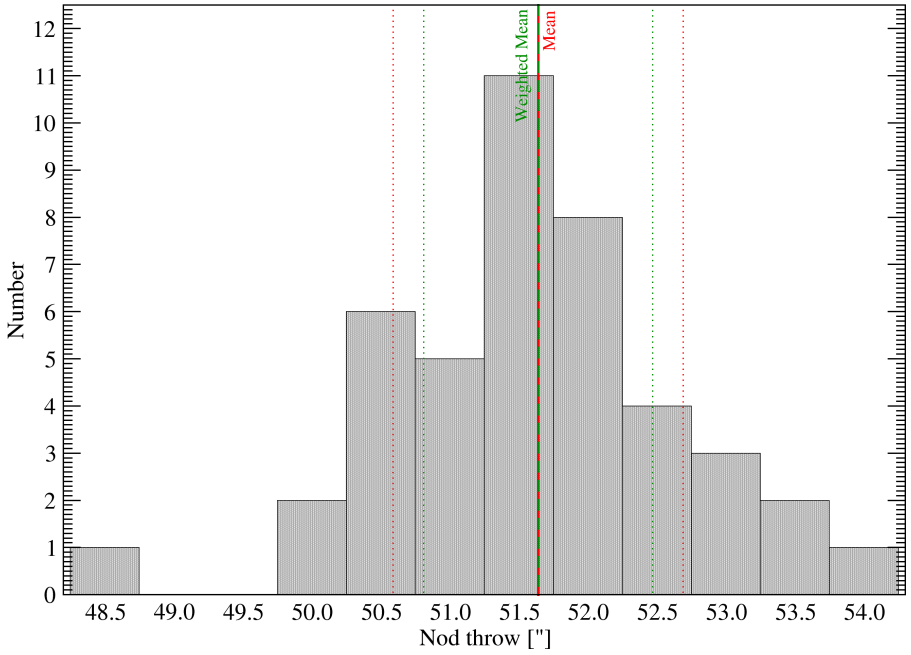

Figure 3: Statistics of the resulting nod throws binned in ranges of 0.5″. The red lines indicate the mean and the standard deviation of the nod throw distribution; the green lines denote the weighted values as given in Tab. 3.

In addition to the usual statistical quantities like mean, median and standard deviation, a statistical analysis was done by weighting the individual results by their uncertainty. The weighted mean $\bar{\theta}_w$ and weighted standard deviation $\sigma_{\theta,w}$ of the nod throw were calculated according to Eqs. 3 and 4. The weights w_i were chosen to be $1/\sigma^2_{\theta,i}$. All numbers of the weighted and unweighted analysis are given in Tab. 3.

Table 2: Selected results of the pointing observation programme of OD 858 after the two-dimensional parameter update of the ACMS. The table lists the STR interlacing status, the RPE (the pointing stability at one nod position), the nod throw θ and its corresponding standard deviation σ_θ. At the bottom, the mean and standard deviation for each of the measured quantities is given.

OBSID	Target	STR Intl	RPE [″]	θ [″]	σ_θ [″]
1342228855	HIP36675	yes	0.20	51.41	0.29
1342228856	HIP30343	no	0.26	50.17	0.47
1342228857	HIP28041	yes	0.39	52.13	0.60
1342228866	HIP30520	no	0.17	51.75	0.26
1342228867	HIP36288	no	0.16	50.73	0.30
1342228868	HIP30945	no	0.23	52.55	0.35
1342228869	HD39741	no	0.42	53.83	0.40
1342228870	HIP75847	no	0.31	52.75	0.28
1342228871	HIP80802	no	0.21	53.22	0.32
1342228872	HIP83866	yes	0.28	52.21	0.35
1342228873	HIP81835	no	0.15	51.61	0.26
1342228874	HIP78574	no	0.21	51.40	0.30
1342228875	HIP80704	no	0.17	52.91	0.36
1342228876	HIP77501	no	0.22	50.85	0.45
1342228877	HIP78235	no	0.21	52.50	0.21
1342228878	HIP79233	no	0.32	50.57	0.32
1342228879	HIP80488	no	0.22	51.66	0.28
1342228880	HIP87747	no	0.29	51.40	0.20
1342228881	HIP84346	no	0.20	52.84	0.33
1342228882	HIP87538	no	0.22	50.45	0.33
1342228883	HIP84780	no	0.37	52.22	0.46
1342228884	HIP79593	no	0.34	53.41	0.77
1342228889	HIP84071	yes	0.23	50.85	0.46
1342228890	HIP82912	no	0.16	51.07	0.28
1342228891	HIP77023	no	0.26	50.82	0.31
1342228892	HIP76377	no	0.25	52.16	0.47
1342228893	HIP82273	no	0.22	50.39	0.28
1342228894	PPM787044	yes	0.20	51.77	0.27
1342228895	HIP68815	no	0.24	51.48	0.29
1342228896	HIP61404	no	0.16	51.78	0.27
1342228897	HIP55355	yes	0.24	50.23	0.49
1342228898	HIP46806	no	0.22	50.66	0.25
1342228899	HIP19424	no	0.26	53.69	0.48
1342228900	HIP31057	no	0.17	51.40	0.27
1342228901	HIP30438	no	0.25	52.59	0.26
1342228902	HIP37819	no	0.36	50.87	0.21
1342228903	HIP35264	yes	0.39	51.69	0.36
1342228904	HD43635	no	0.17	51.69	0.26
1342228905	HIP28874	yes	0.24	51.58	0.20
1342228906	HIP28816	no	0.18	50.71	0.29
1342228907	HIP30800	no	0.18	51.97	0.23
1342228915	HIP30326	no	0.19	52.12	0.21
1342228916	HIP32923	no	0.32	48.53	0.64
Mean			0.24	51.64	0.34
Standard deviation			0.07	1.05	0.12

$$\bar{\theta}_w = \frac{\sum_{i=1}^{n} w_i \theta_i}{\sum_{i=1}^{n} w_i} \tag{3}$$

$$\sigma^2_{\theta,w} = \frac{\sum_{i=1}^{n} w_i}{\left(\sum_{i=1}^{n} w_i\right)^2 - \sum_{i=1}^{n} w_i^2} \sum_{i=1}^{n} w_i \left(\theta_i - \bar{\theta}_w\right)^2 \tag{4}$$

Table 3: Overall statistical properties of the nod throws determined from the individual measurements. The weighted numbers were calculated according to Eqs. 3 and 4.

	unweighted [″]	weighted [″]
mean	51.64	51.64
median	51.66	–
standard deviation	1.05	0.83

5 Conclusions

This report investigates the relative pointing performance of the Herschel telescope after the two-dimensional STR focal length parameter update of the ACMS done on OD 858. The SRPE cannot be derived from these observations, because it is not defined for the *basic_fine_pointing* mode used for the chopped/nodded observations of the PACS instrument. Instead, we define a pseudo SRPE (pSRPE) as the APE of small telescope displacements as they are attained during such observations. In practice, such a redefinition is irrelevant for many of the applications, because at least the chopped/nodded observations are affected by just this uncertainty and not the proper SRPE that affects raster observations. In this respect, the relevance of the SRPE and the pSRPE can be exchanged. Since the individual measurements only consist of one nod cycle, the uncertainty of the nod throw during one observation is mainly determined by the RPE. In this analysis, the nod throw uncertainty per observation turns out to be $0.34'' \pm 0.12''$.

Instead, the full ensemble is used as a more representative measure of the pSRPE as if it comprised a single measurement with 43 AB nod cycle patterns. The derived nod throws are affected both by the pointing stability at one nod position, the RPE, and the accuracy of the telescope movement between the nod cycles, the pSRPE. Therefore, the statistics of the nod throws can be used for deriving an approximate value of the pSRPE.

Altogether, we find that the reproducibility of the nod throw is of the same order as the newly determined APE. The mean nod throw of all 43 observations was $51.64''$ with a scatter of $1.05''$. If an equally weighted contribution of the RPE ($0.24'' \pm 0.07''$) and the pSRPE to the nod throw reproducibility is assumed, the pSRPE would be

$$pSRPE = \sqrt{(1.05'')^2 - (0.24'')^2} = 1.02'' \tag{5}$$

This means that by exchanging the pointing mode for chopped/nodded observations from *basic_raster_pointing* to *basic_fine_pointing*, the pSRPE fulfils the requirement of the original SRPE. This result also shows that the pSRPE is of the same order as the APE. After weighing the individual results with the corresponding standard deviations, the weighted mean becomes $51.64''$ with an unbiased weighted standard deviation of $0.83''$. Based on this calculation, the pSRPE would have a value of $0.79''$.

These numbers are very promising. It remains to be verified, if the chopped/nodded PACS spectroscopy observations really benefit from this pointing improvement. If the line and continuum fluxes turn out to be more stable and reliable than before, all the efforts made to achieve a better behaving ACMS providing an improved APE would have been justified also from this perspective.